

NONLINEAR DISTURBANCE OBSERVER-BASED FAST TERMINAL SLIDING MODE GUIDANCE LAW WITH IMPACT ANGLE CONSTRAINTS

JUNHONG SONG, SHENMIN SONG, YONG GUO AND HUIBO ZHOU

Center for Control Theory and Guidance Technology
Harbin Institute of Technology
No. 92, West Dazhi Street, Harbin 150001, P. R. China
hitsjh@163.com; songshenmin@hit.edu.cn; guoyonghit@126.com; zhouhb0306@sina.com

Received June 2014; revised October 2014

ABSTRACT. *For the terminal guidance problem of tactical missiles intercepting maneuvering targets with impact angle constraints, a fast terminal sliding mode guidance law without any singularity is proposed based on a nonlinear disturbance observer. Considering the target acceleration as an unknown bounded external disturbance, the nonlinear disturbance observer is employed to estimate the external disturbance. The estimated disturbance is used to compensate the actual disturbance, which aims to alleviate the chattering and to make the proposed guidance law with stronger robustness. With the aid of the Lyapunov stability theory, the finite time convergence of the line-of-sight angle and the line-of-sight angular rate in both reaching and sliding phase is proven based on a fast terminal sliding mode and a switching controller that eliminates the singularity problem generated by the fast terminal sliding mode control. Numerical simulations are presented to demonstrate the effectiveness of the proposed guidance law. Although the proposed guidance law is developed under the assumption that the missile speed is a constant, the simulation results for the time-varying speed of missiles are also presented to validate the proposed guidance law further.*

Keywords: Missile, Guidance law, Finite time convergence, Fast terminal sliding mode, Nonlinear disturbance observer

1. Introduction. The main purpose of a missile guidance law is to guide missiles to intercept targets with minimal miss distances. In current applications, to increase the effectiveness of warheads against targets and achieve the best destroying effect [1], a specific terminal impact angle needs to be considered. Therefore, to meet the requirement of this special guidance mission, it is necessary to do a further study on the guidance law with terminal impact angle constraints. At present, many researchers have developed a variety of guidance laws with impact angle constraints, which are based on proportional navigation [2,3], optimal control [4,5], differential game [6,7] and sliding mode control [8-11], etc.

It is well known that the sliding mode control (SMC) has good robustness to external disturbances and parametric uncertainties [12-14]. The basic idea of the SMC is to drive the system states to the designed sliding mode surface, and then to maintain the system states on the sliding mode surface so that the desired convergence property of system states can be obtained in the sliding phase. In the literature, the traditional linear SMC can only finish the asymptotic convergence in the sliding phase [15,16]. In order to achieve the finite time convergence in the sliding phase, the terminal sliding mode control (TSMC) was proposed in [17] for rigid robotic manipulators. Compared with the conventional linear SMC, the TSMC can provide a faster convergence rate and a higher control precision.

This initial TSMC has been widely applied in missile guidance law design [11,18,19]. However, the initial TSMC results in two disadvantages. The first one is the singularity problem. For example, these guidance laws proposed in [11,18,19] had the singularity problem. In order to resolve the singularity problem, nonsingular terminal sliding mode control (NTSMC) was developed in [20-22]. Various NTSMC algorithms could be divided into two types. One is to design a novel nonsingular sliding mode surface directly based on the system states. This NTSMC method has been successfully used for the guidance law design with the impact angle constraints [23-25]. The other is to develop the switching controller to avoid the singularity [21,22]. The second problem is that it has a slower convergence rate than the traditional linear SMC when the system state is far away from the equilibrium. To overcome the second problem, two fast terminal sliding mode controls (FTSMC) combining the advantages of linear SMC and TSMC were given in [26] and [27].

As we all know, in the implementation of the sliding mode control, there exists an unavoidable chattering problem. In order to alleviate the chattering phenomenon and improve the system performance, an efficient method is to estimate the disturbances by employing a disturbance observer (DOB). The DOB technique was first proposed in [28]. Since then, various disturbance observers have been developed and applied in many control fields [29-31]. Up to now, DOB-based guidance laws have been designed in much literature. For example, in [32], for the missile guidance law design, an extended state observer was designed to estimate the target's acceleration viewed as the external disturbance. An extended high-gain observer was put forward to estimate unknown disturbance precisely in [33]. In [34], a nonlinear disturbance observer was proposed and used to design the guidance law with impact angle constraint and autopilot lag. The above-mentioned DOB can estimate the unknown disturbance precisely; however, the result is not finite time convergence. [35] proposed a nonlinear disturbance observer (NDOB), which is able to perform transient estimation with high precision for the disturbance in the finite time. However, this method converges quite slowly when there is great initial error, which is determined by the nature of homogeneous system. Based on the proposed NDOB in [35], [36] proposed a novel NDOB to speed up the transient process in finite time.

This paper investigates the terminal guidance problem for the tactical missiles intercepting the maneuvering targets with impact angle constraints in the presence of bounded external disturbances. With the purpose of addressing the above-mentioned problems generated by the initial TSMC and by considering the target acceleration as unknown external disturbances, this paper proposes a new NDOB-based nonsingular fast terminal sliding mode guidance law. Compared with the listed literature, the main contributions of this paper are as follows. (1) The proposed guidance law not only avoids the singularity problem but also improves the convergence rate when the guidance system states are far away from the equilibrium. (2) By use of the NDOB, the target acceleration viewed as the external disturbance can be estimated precisely in finite time. So, the knowledge of the target acceleration is not required to be known in advance. (3) The proposed guidance law can guarantee the finite-time convergence of the line-of-sight (LOS) angle and the LOS angular rate in both the reaching phase and the sliding phase by a Lyapunov-based approach. And, both the LOS angle and the LOS angular rate can fast converge to their corresponding desired value in finite time.

This paper is organized as follows. Some preliminaries are briefly stated in the following section. In Section 3, firstly, an NDOB is introduced to estimate the target's acceleration. Then, a novel NDOB-based fast terminal sliding mode guidance law with impact angle constraints is proposed and the corresponding stability proofs are given as well. In Section 4, simulation results are presented, which are used to verify the effectiveness of the proposed guidance law. The last section concludes this paper.

2. Problem Formulation. This section presents the equations of guidance system for the missile intercepting the target. For simplicity, only a two-dimensional model is considered. The engagement geometry of a missile and a target is shown in Figure 1, in which the missile and the target are regarded as point masses, respectively. We assume that the velocities of the missile and the target are constants, and the autopilot is fast enough to be neglected. Under these assumptions, the corresponding equations of motion can be described by the following differential equations:

$$\dot{r} = V_t \cos(q - \varphi_t) - V_m \cos(q - \varphi_m) \tag{1}$$

$$r\dot{q} = -V_t \sin(q - \varphi_t) + V_m \sin(q - \varphi_m) \tag{2}$$

$$\dot{\varphi}_t = \frac{a_t}{V_t} \tag{3}$$

$$\dot{\varphi}_m = \frac{a_m}{V_m} \tag{4}$$

where r and \dot{r} denote the relative distance and the relative velocity from the missile to the target, respectively; V_t and V_m represent the velocities of the target and the missile, respectively; q and \dot{q} denote the line-of-sight (LOS) angle and LOS angular rate between the missile and the target, respectively; φ_t and φ_m represent the flight path angles of the target and the missile, respectively; a_m and a_t are the lateral accelerations of the missile and the target, respectively.

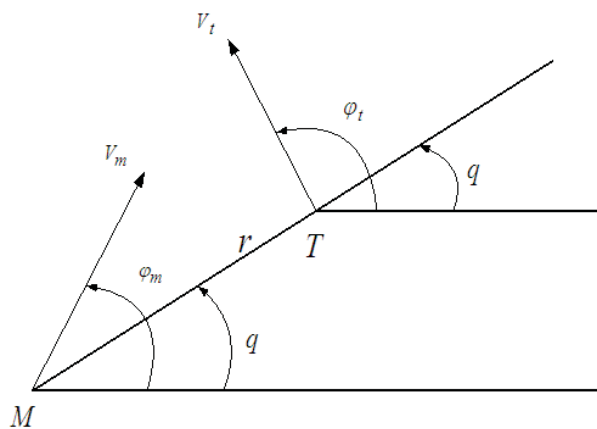


FIGURE 1. Two-dimensional engagement geometry

By differentiating (2) with respect to time and using (1), (3) and (4), we can get

$$\ddot{q} = -\frac{2\dot{r}}{r}\dot{q} - \frac{\cos(q - \varphi_m)}{r}a_m + \frac{\cos(q - \varphi_t)}{r}a_t \tag{5}$$

Note that, because the missile lateral acceleration a_m is multiplied by the term $\cos(q - \varphi_m)$, the LOS angle q can be controlled when $|q - \varphi_m| \neq \frac{\pi}{2}$. In [11], it has been proved that, if $|q - \varphi_m| = \frac{\pi}{2}$, then $\dot{q} - \dot{\varphi}_m \neq 0$. Therefore, $|q - \varphi_m| = \frac{\pi}{2}$ is not a stable equilibrium point and, as a result, the missile lateral acceleration a_m can be used to control the LOS angle q . By [11], we can see that the issue of impact angle control can be converted into the issue of terminal LOS angle control.

This paper aims at developing a guidance law a_m such that the guidance law a_m could not only guarantee that the missile has a small miss distance, but also ensure that the LOS angular rate \dot{q} converges to zero in finite time, and the LOS angle q converges to the desired terminal LOS angle q_d in finite time in the presence of external disturbance.

In this paper, required dates such as q , \dot{q} , r , \dot{r} and φ_m are available. Let q_d be pre-specified with a constant value. Define $x_1 = q - q_d$ and $x_2 = \dot{q}$. Substituting them into (5) yields

$$\begin{cases} \dot{x}_1 = x_2 \\ \dot{x}_2 = f + ba_m + d \end{cases} \quad (6)$$

where $f = -\frac{2\dot{r}}{r}x_2$, $b = -\frac{\cos(q - \varphi_m)}{r}$, $d = \frac{\cos(q - \varphi_t)}{r}a_t$.

Remark 2.1. [37] *Let the starting time of the terminal guidance process be zero. During the guiding process, it has $\dot{r}(t) < 0$, $0 < r(t) < r(0)$, $t > 0$.*

Remark 2.2. [35] *Technically, the missile intercepting target by impact ("hit-to-kill") happens when $r \neq 0$ but belongs to the interval $r_0 \in [r_{\min}, r_{\max}] = [0.1, 0.25]m$. Therefore, during the whole interception process, the inequality holds.*

$$r_0 \leq r(t) \leq r(0) \quad (7)$$

In practical applications, the target acceleration is regarded as external disturbance, and it is usually difficult to obtain. However, it has upper bound. Referring to Remark 2.2, we have the following assumption.

Assumption 2.1 *d is regarded as lumped external disturbance and assumed to be bounded satisfying $|d| \leq \Delta$, where Δ is a positive constant.*

3. Design of the NDOB-based Fast Terminal Sliding Mode Guidance Law.

3.1. Nonlinear disturbance observer. Consider single-input and single-output (SISO) dynamics of the first order

$$\dot{\zeta} = g(t) + u \quad (8)$$

where $\zeta \in R^1$, $u \in R^1$ is a control input, $g(t)$ is a sufficiently smooth uncertain function. Let the variables ζ and u be obtained in real time, $g(t)$ satisfies $\dot{g}(t) \leq L$, $L > 0$ is a Lipschitz constant. The control input function u is Lebesgue-measurable. Equation (8) is understood in the Filippov sense [38], which implies in particular that $\zeta(t)$ is an absolutely continuous function for $\forall t \geq 0$. By modifying of the NDOB in [36] simply, the following result is obtained.

Lemma 3.1. (See [36]) *Consider the following NDOB:*

$$\begin{cases} \dot{z}_0 = v_0 + u \\ v_0 = -\lambda_2 L^{\frac{1}{3}} |z_0 - \zeta|^{\frac{2}{3}} \text{sign}(z_0 - \zeta) - \mu_2(z_0 - \zeta) + z_1 \\ \dot{z}_1 = v_1 \\ v_1 = -\lambda_1 L^{\frac{1}{2}} |z_1 - v_0|^{\frac{1}{2}} \text{sign}(z_1 - v_0) - \mu_1(z_1 - v_0) + z_2 \\ \dot{z}_2 = -\lambda_0 L \text{sign}(z_2 - v_1) - \mu_0(z_2 - v_1) \end{cases} \quad (9)$$

where $\lambda_i, \mu_i > 0$, $i = 0, 1, 2$ are chosen sufficiently large values in the reverse order, and then it can be given that z_1 converges to $g(t)$ in finite time.

Guidance system (6) can be rewritten as

$$\begin{cases} \dot{x}_1 = x_2 \\ \dot{x}_2 = h(t) + ba_m \end{cases} \quad (10)$$

where $h(t) = f + d = -\frac{2\dot{r}}{r}x_2 + \frac{\cos(q - \varphi_t)}{r}a_t$. The derivative of function $h(t)$ is

$$\dot{h}(t) = \frac{1}{r^2}[2\dot{r}^2x_2 - 2r\ddot{r}x_2 - 2r\dot{r}\dot{x}_2] + \frac{1}{r^2}[(r\dot{a}_t - \dot{r}a_t)\cos(q - \varphi_t) - r(\dot{q} - \dot{\varphi}_t)a_t\sin(q - \varphi_t)] \quad (11)$$

Remark 3.1. *If the target acceleration a_t is differentiable, then the function $h(t)$ is also differentiable except for $r = 0$. According to Remark 2.2, the function $h(t)$ is differentiable and the function $\dot{h}(t)$ is continuous everywhere until hit-to-kill happens. Therefore, the function $h(t)$ is continuously differentiable for any $r \geq r_0$, the function $\dot{h}(t)$ has a Lipschitz constant L .*

For the guidance system (6), according to Lemma 3.1 and Remark 3.1, the lumped external disturbance d can be estimated by the following NDOB (12)

$$\begin{cases} \dot{z}_0 = v_0 + f + ba_m \\ v_0 = -\lambda_2 L^{\frac{1}{3}} |z_0 - x_2|^{\frac{2}{3}} \text{sign}(z_0 - x_2) - \mu_2(z_0 - x_2) + z_1 \\ \dot{z}_1 = v_1 \\ v_1 = -\lambda_1 L^{\frac{1}{2}} |z_1 - v_0|^{\frac{1}{2}} \text{sign}(z_1 - v_0) - \mu_1(z_1 - v_0) + z_2 \\ \dot{z}_2 = -\lambda_0 L \text{sign}(z_2 - v_1) - \mu_0(z_2 - v_1) \\ \hat{d}(t) = z_1 \end{cases} \quad (12)$$

where $\hat{d}(t)$ is the estimated lumped external disturbance. According to Lemma 3.1, we can obtain that the estimated lumped external disturbance $\hat{d}(t)$ converges to the real lumped external disturbance $d(t)$ in finite time.

3.2. Guidance law design. Before designing the guidance law, the following assumption is presented on the basis of Lemma 3.1.

Assumption 3.1. *The lumped external disturbance estimation error is bounded and there exists a known positive constant Δ_{\max} , such that*

$$|d(t) - \hat{d}(t)| \leq \Delta_{\max} \quad (13)$$

The following lemma is useful for the stability analysis of the guidance system.

Lemma 3.2. [27] *Suppose that there exists a continuous positive definite function $V(t)$, and that $\dot{V}(t) \leq -\alpha_1 V(t) - \alpha_2 V(t)^\eta, \forall t > t_0$, where $\alpha_1 > 0, \alpha_2 > 0$ and $0 < \eta < 1$. Then, the system state converges to the equilibrium point in finite time. The setting time can be given by $t_f \leq t_0 + \frac{1}{\alpha_1(1-\eta)} \ln \frac{\alpha_1 V(t_0)^{1-\eta} + \alpha_2}{\alpha_2}$.*

In order to make x_1 and x_2 converge to zero fast along the sliding mode surface in finite time, a fast terminal sliding mode manifold [27] based on the guidance system states can be described by the following equation:

$$s = x_2 + \alpha x_1 + \beta \text{sig}(x_1)^\gamma \quad (14)$$

where $\text{sig}(x_1)^\gamma = |x_1|^\gamma \text{sign}(x_1), \frac{1}{2} < \gamma < 1, \alpha$ and β are positive constants.

Based on the fast terminal sliding mode manifold (14) and motivated by [22], the guidance law without singularity is designed as follows:

$$a_m = \frac{-f - (\alpha x_2 + \text{sat}(\beta\gamma |x_1|^{\gamma-1} x_2, a_0)) - k_1 s - k_2 \text{sign}(s) - \hat{d}(t)}{b} \quad (15)$$

where

$$\text{sat}(\beta\gamma |x_1|^{\gamma-1} x_2, a_0) = \begin{cases} \beta\gamma |x_1|^{\gamma-1} x_2, & \beta\gamma |x_1|^{\gamma-1} |x_2| \leq a_0 \\ a_0 \text{sign}(x_2), & \beta\gamma |x_1|^{\gamma-1} |x_2| > a_0 \end{cases} \quad (16)$$

$k_2 = \varepsilon + \Delta_{\max}, \varepsilon, k_1$ and a_0 are positive constants.

Then we obtain the following theorem.

Theorem 3.1. *For the guidance system (6) with the fast terminal sliding mode manifold (14), if the guidance law is chosen as (15), then the states of the guidance system (6) can reach the fast terminal sliding mode surface $s = 0$ in finite time. Furthermore, the LOS angle q converges to the desired LOS angle q_d in finite time, and the LOS angle rate \dot{q} converges to zero in finite time.*

Proof: We choose the following positive function as a Lyapunov function

$$V_1 = \frac{1}{2}s^2 \tag{17}$$

Applying (6), (14) and (15), the time derivative of V_1 can be written as

$$\begin{aligned} \dot{V}_1 &= s\dot{s} \\ &= s(\dot{x}_2 + \alpha x_2 + \beta\gamma|x_1|^{\gamma-1}x_2) \\ &= -k_1s^2 - k_2|s| + (d(t) - \hat{d}(t))s + s(\beta\gamma|x_1|^{\gamma-1}x_2 - \text{sat}(\beta\gamma|x_1|^{\gamma-1}x_2, a_0)) \\ &\leq -k_1s^2 - \varepsilon|s| + s(\beta\gamma|x_1|^{\gamma-1}x_2 - \text{sat}(\beta\gamma|x_1|^{\gamma-1}x_2, a_0)) \end{aligned} \tag{18}$$

In order to prove the theorem conveniently, we divide the space $[x_1, x_2]^T \in R^2$ into two areas named as A and B , which are described respectively as follows:

$$A = \{(x_1, x_2) : \beta\gamma|x_1|^{\gamma-1}|x_2| \leq a_0\} \tag{19}$$

$$B = \{(x_1, x_2) : \beta\gamma|x_1|^{\gamma-1}|x_2| > a_0\} \tag{20}$$

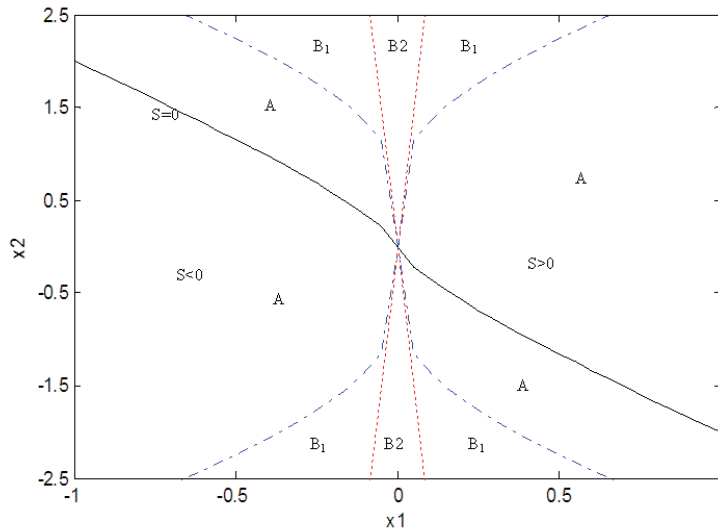


FIGURE 2. Singular and nonsingular areas ($\alpha = \beta = 1, \gamma = 0.6, a_0 = 2$)

From Figure 2, we can observe that s always stays in the area A and crosses the area B only in the origin. When $s = x_2 + \alpha x_1 + \beta\text{sig}(x_1)^\gamma = 0$, we have $x_2 = -\alpha x_1 - \beta\text{sig}(x_1)^\gamma$. Further, because of $\frac{1}{2} < \gamma < 1$, it can be obtained that $\lim_{x_1 \rightarrow 0, x_2 \rightarrow 0} |x_1|^{\gamma-1}x_2 = 0$, along $s = 0$. Therefore, after the guidance system states reach to the fast terminal sliding mode surface, there is no singularity problem.

When the guidance system states are in A , the saturation function Equation (16) can be rewritten as Equation (21).

$$\text{sat}(\beta\gamma|x_1|^{\gamma-1}x_2, a_0) = \beta\gamma|x_1|^{\gamma-1}x_2 \tag{21}$$

Then, using Equations (18) and (21), we have

$$\dot{V}_1 \leq -k_1 s^2 - \varepsilon |s| = -2k_1 V_1 - \sqrt{2\varepsilon} V_1^{\frac{1}{2}} \tag{22}$$

According to Lemma 3.2, we can obtain that the existence condition of the fast terminal sliding mode holds for the guidance system (6) and further the fast terminal sliding mode surface s can converge to zero in finite time.

When the guidance system states are in the area B , it can be obtained that

$$\text{sat}(\beta\gamma |x_1|^{\gamma-1} x_2, a_0) = a_0 \text{sign}(x_2) \tag{23}$$

Applying Equations (14), (15) and (23), we can obtain

$$\dot{s} = -k_1 s - k_2 \text{sign}(s) - a_0 \text{sign}(x_2) + (d(t) - \hat{d}(t)) + \beta\gamma |x_1|^{\gamma-1} x_2 \tag{24}$$

When x_1 approaches zero, from Equation (24), we have $\dot{s} = O(\beta\gamma |x_1|^{\gamma-1} x_2)$ as $x_1 \rightarrow 0$ subject to $x_2 \neq 0$, where O is a Landau symbol representing the complexity function. Then, we can obtain

$$\begin{aligned} \dot{V}_1 &= sO(\beta\gamma |x_1|^{\gamma-1} x_2) \\ &= (x_2 + \alpha x_1 + \beta \text{sig}(x_1)^\gamma)O(\beta\gamma |x_1|^{\gamma-1} x_2) \\ &= O(\beta\gamma |x_1|^{\gamma-1} x_2^2) \end{aligned} \tag{25}$$

Therefore, as $x_1 \rightarrow 0$ subject to $x_2 \neq 0$, we have $\dot{V}_1 > 0$.

Based on the above analysis, we can divide the area B into two areas, B_1 and B_2 shown in Figure 2, which are defined as follows:

$$B = B_1 \vee B_2 \tag{26}$$

$$B_1 = \{(x_1, x_2) : \dot{V}_1 < 0\} \tag{27}$$

$$B_2 = \{(x_1, x_2) : \dot{V}_1 > 0\} \tag{28}$$

So, in the area B_1 , the same with that in the area A , the existence condition of the fast terminal sliding mode still holds. However, when the guidance system states are in the area B_2 , the guidance system does not satisfy the existence condition of the fast terminal sliding mode.

When guidance system states move to B from A , saturation function $\text{sat}(\beta\gamma |x_1|^{\gamma-1} x_2, a_0)$ will change to $a_0 \text{sign}(x_2)$ from $\beta\gamma |x_1|^{\gamma-1} x_2$. In the area B_1 , $\dot{V}_1 < 0$ still holds, that is, the existence condition of the sliding mode still holds. However, when the guidance system states further enter B_2 from B_1 , that is, x_1 approaches zero. As $x_1 \rightarrow 0$ and $x_2 \neq 0$, the guidance system does not satisfy the existence condition of the sliding mode. Owing to the external disturbance in the guidance system (6), it is hard to determine the boundary exactly between B_1 and B_2 . However, it does not affect the proof.

From the guidance system (6), the solution for $x_1(t)$ can be described as

$$x_1(t) = x_1(0) + \int_0^t x_2(t) dt \tag{29}$$

Using Equations (6), (15) and (16), we have

$$\dot{x}_2 = -\alpha x_2 - a_0 \text{sign}(x_2) - k_1 s - k_2 \text{sign}(s) + (d(t) - \hat{d}(t)) \tag{30}$$

When the guidance system states are in the area B , we can divide the guidance system states into two different cases. In case 1, we have $x_2 > 0$; in case 2, we have $x_2 < 0$.

When $x_2 > 0$, from Equation (29), we can obtain that x_1 increases monotonically till reaching and crossing the boundary between A and B in the single direction of increasing x_1 . In addition, from Equation (30), we have $\dot{x}_2 < 0$.

Similarly, when $x_2 < 0$, it can be seen that x_1 decreases monotonically till reaching and crossing the boundary between A and B in the single direction of decreasing x_1 , and $\dot{x}_2 > 0$.

Therefore, the guidance system states will not stay in the area B forever, but cross from B to A in finite time. Once the guidance system states enter A , the guidance system states will stay in A and satisfy the existence condition of the sliding mode. Therefore, from Equation (22) the states of the guidance system (6) can reach the fast terminal sliding mode surface $s = 0$ in finite time.

In the end, we prove that the guidance system states converge to zero in finite time after reaching the fast terminal sliding mode surface.

In the sliding phase $s = 0$, the following equation is given

$$x_2 + \alpha x_1 + \beta \text{sig}(x_1)^\gamma = 0 \quad (31)$$

Choose the following Lyapunov function

$$V_2 = \frac{1}{2}x_1^2 \quad (32)$$

By differentiating V_2 with respect to time and applying Equation (32), we have

$$\begin{aligned} \dot{V}_2 &= x_1 \dot{x}_1 \\ &= -\alpha x_1^2 - \beta |x_1|^{\gamma+1} \\ &= -2\alpha V_2 - (\sqrt{2})^{\gamma+1} \beta V_2^{\frac{\gamma+1}{2}} \end{aligned} \quad (33)$$

By Lemma 3.2, the guidance system states x_1 and x_2 converge to zero in finite time. Hence, the LOS angle q converges to the desired LOS angle q_d in finite time, and the LOS angular rate \dot{q} converges to zero in finite time. This completes the proof.

Remark 3.2. In order to guarantee that the fast terminal sliding mode surface $s = 0$ lies in A rather than B as shown in Figure 2, a_0 can be selected as $\beta\gamma\alpha x_{1\max}^\gamma + \beta^2\gamma x_{1\max}^{2\gamma-1} < a_0$, where the bounded constant $x_{1\max}$ is defined as $|x_1| < x_{1\max}$.

Because of the signum function in Equation (15), the proposed guidance law is a non-smooth controller which can induce the chattering problem. In order to remove the chattering, the signum function is replaced with a saturation function $\text{sat}(s)$. Hence, the proposed guidance law in Equation (15) is modified as

$$a_m = \frac{-f - (\alpha x_2 + \text{sat}(\beta\gamma|x_1|^{\gamma-1}x_2, a_0)) - k_1s - k_2\text{sat}(s) - \hat{d}(t)}{b} \quad (34)$$

with

$$\text{sat}(s) = \begin{cases} 1, & s > h \\ s/h, & |s| \leq h \\ -1, & s < -h \end{cases} \quad (35)$$

where h is a small positive constant.

4. Simulation Results. In this section, the simulation results illustrating the effectiveness of the proposed guidance law (34) used for the tactical missiles air-intercepting maneuvering target are presented. First, we present the comparison between the proposed guidance law in this paper and the existing ones for the constant speed missile against the different kinds of maneuvering targets. Then, a case of the time-vary speed missiles intercepting the targets is considered to verify the advantage of the proposed guidance law further.

The initial conditions of the guidance system are chosen as follows. The initial relative distance between the missile and the target is $r(0) = 5000\text{m}$. The initial LOS angle is $q(0) = 30\text{deg}$. The desired LOS angle is $q_d = 20\text{deg}$. The missile's velocity is $V_m = 600\text{m/s}$ and its initial flight path angle is $\varphi_m(0) = 60\text{deg}$. The target's velocity is $V_t = 300\text{m/s}$ and its initial flight path angle is $\varphi_t(0) = 0\text{deg}$. The parameters of guidance law (34) are chosen as $\alpha = 10$, $\beta = 5$, $\gamma = 3/4$, $k_1 = 0.5$, $k_2 = 0.01$, $a_0 = 5$, $h = 0.002$. The parameters of NDOB are selected as $\lambda_0 = 1.1$, $\lambda_1 = 1.5$, $\lambda_2 = 2$, $\mu_0 = 3$, $\mu_1 = 6$, $\mu_2 = 8$, $L = 100$. The maximal acceleration of the missile is $40g$, and g is the acceleration of gravity ($g = 9.8\text{m/s}^2$).

4.1. Constant speed missiles. In the subsection, the simulation results for the constant speed missile intercepting two different target acceleration profiles are presented.

In order to verify the effectiveness of the proposed guidance law, two different target acceleration profiles, which are cosine maneuvering and step maneuvering, are considered as those given below.

- 1) Case 1. $a_t = 7g \cos(\pi t/4)\text{m/s}^2$.
- 2) Case 2. $a_t = 7g\text{m/s}^2$ for $t < 5\text{s}$ and $a_t = -7g\text{m/s}^2$ for $t \geq 5\text{s}$.

For performance comparison, the traditional PN guidance law and the adaptive non-singular terminal sliding mode guidance law [25] are also simulated under the same conditions. The traditional PN guidance law is chosen as $a_m = -N\dot{r}\dot{q}$, where the parameter N is set to be 4. In [25], the guidance law is designed as

$$s = x_1 + \alpha |x_2|^{\frac{p}{q}} \text{sgn}(x_2) \tag{36}$$

$$a_m = \frac{r}{\cos(q - \varphi_m)} \left[-\frac{2\dot{r}\dot{q}}{r} + \frac{q}{\alpha p} |x_2|^{2-\frac{p}{q}} \text{sgn}(x_2) + \frac{\hat{\Delta}\rho\text{sat}(s)}{r} + \frac{K\text{sat}(s)}{r} \right] \tag{37}$$

where

$$\text{sat}(s) = \begin{cases} \text{sgn}(s), & |s| > \delta \\ \frac{s}{\delta}, & |s| \leq \delta \end{cases} \tag{38}$$

$$\hat{\Delta} = \begin{cases} \alpha\rho\frac{p}{qr} |x_2|^{\frac{p}{q}-1} |s|, & |s| \geq v \\ 0, & |s| < v \end{cases} \tag{39}$$

Parameters are

$$\alpha = 1, p = 7, q = 5, K = 1800, v = 0.05, \delta = 0.01, \rho = 2, \hat{\Delta}(0) = 100$$

For simplicity, we denote the proposed guidance law in this paper, the PN guidance law and the guidance law in [25] as the D-NFTSM, PNG and ANTSM, respectively.

With the initial conditions and data given above, simulations are performed for the target acceleration profiles of case 1 and case 2. Simulation results are shown in Figures 3 and 4, respectively. Each figure consists of the responses of LOS angle, LOS angular rate, sliding mode manifold, missile acceleration command, estimation error of lumped disturbance and trajectories of the missile and the target for all the three guidance laws, which are given in Figures (a)-(f), respectively. The miss distances and interception times are shown in Table 1.

From Figures 3(a) and 4(a), we can observe that the proposed D-NFTSM guidance law and the ANTSM guidance law can guarantee the LOS angles converge to the desired LOS angle in finite time for the target acceleration profiles of case 1 and case 2. However, under the D-NFTSM guidance law the convergence speed of the LOS angle is much faster and the curve of the LOS angle is smoother than that under the ANTSM guidance law in each one of the two cases. It can also be seen that the LOS angle under the PN

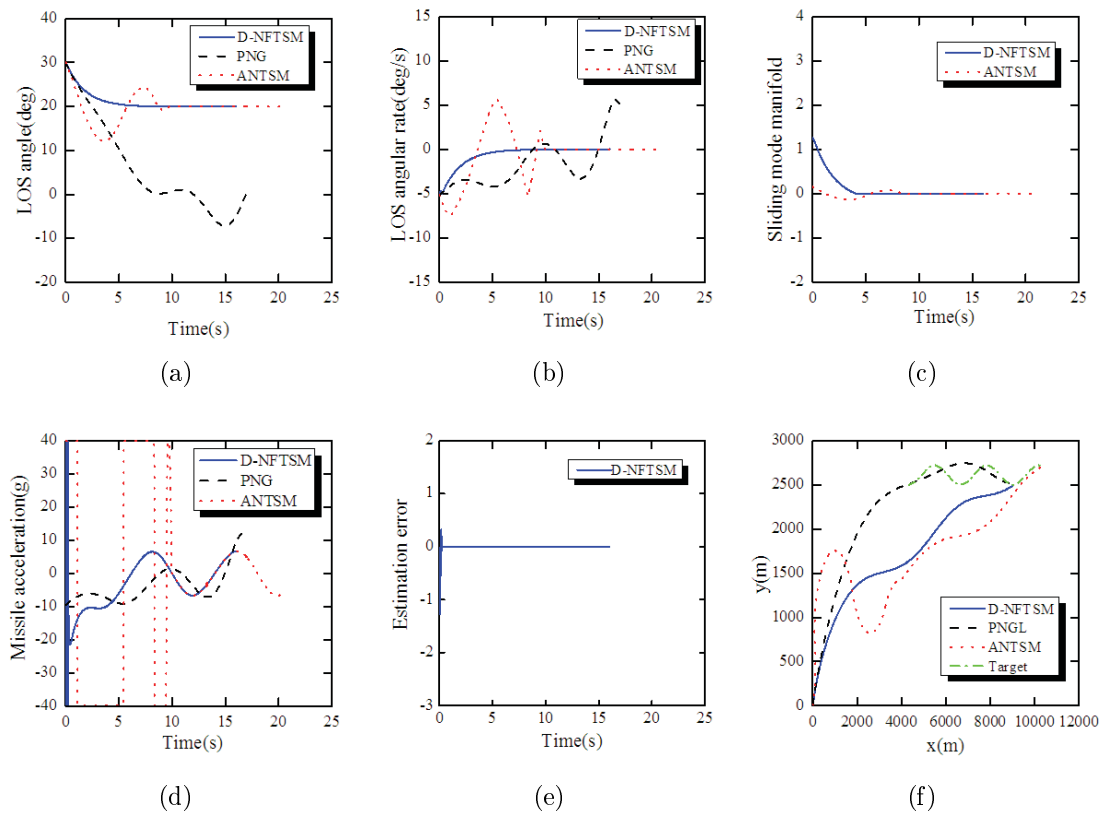


FIGURE 3. Responses under three guidance laws in case 1: (a) LOS angle; (b) LOS angular rate; (c) Sliding mode manifold; (d) Missile acceleration command; (e) Estimation error of disturbance; (f) Trajectories of missile and target

guidance law will not converge for case 1 and case 2. As shown in Figures 3(b) and 4(b), the LOS angular rate under the PN guidance law will not converge for the all target acceleration cases, while both the proposed D-NFTSM guidance law and the ANTSM guidance law are able to make the LOS angular rates reach to zero in finite time, no matter whether the cosine maneuvering target or the step maneuvering target. Especially, the convergence speed of the LOS angular rate under the proposed D-NFTSM guidance law is significantly superior to that under the ANTSM guidance law. At the same time, it can also be observed that the LOS angular rate under the ANTSM guidance law oscillates around zero until it converges to zero for each case. However, the LOS angular rate of the D-NFTSM guidance law fast converges to zero smoothly. Figures 3(c) and 4(c) depict the convergence performance of sliding mode manifold. It can be seen that the sliding mode manifold under the proposed guidance law converges to zero in finite time (in approximately 4s) for the two cases, whose convergence speed is faster than that under the ANTSM guidance law. From the convergence time of the LOS angle and sliding mode manifold with the proposed D-NFTSM guidance law, it is obvious that the desired LOS angle is achieved in finite time with the proposed guidance law after occurrence of the sliding mode surface.

We can observe from Figures 3(d) to 4(d) that the missile lateral accelerations under all the three guidance laws are within the reasonable bounds. And, at the start of the engagement, the missile acceleration generated by the proposed D-NFTSM guidance law is larger than that of the PN guidance law for the target acceleration profiles of case 1

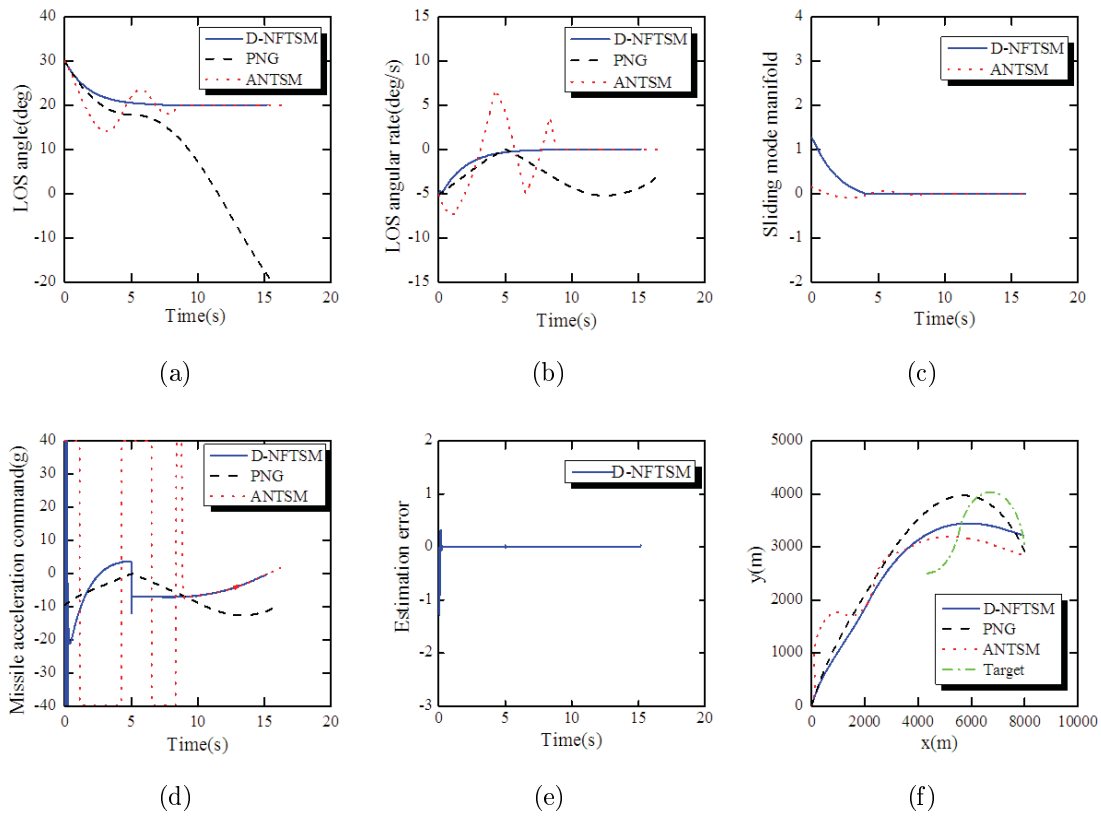


FIGURE 4. Responses under three guidance laws in case 2: (a) LOS angle; (b) LOS angular rate; (c) Sliding mode manifold; (d) Missile acceleration command; (e) Estimation error of disturbance; (f) Trajectories of missile and target

TABLE 1. Miss distances and interception times

Guidance laws	Case 1		Case 2	
	Miss distance (m)	Interception time (s)	Miss distance (m)	Interception time (s)
D-NFTSM	0.060	16.040	0.075	15.180
PNG	1.160	17.101	3.073	16.310
ANTSM	0.11	20.552	0.137	16.512

and case 2. However, the larger missile acceleration in the initial time under the proposed guidance law can make the LOS angle and LOS angular rate preferably converge to the desired values, respectively. In addition, it is obvious that the proposed guidance law does not bring about the chattering and singularity. However, owing to the oscillating of the LOS angular rate under the ANTSM guidance law in the first 10 seconds, the corresponding missile acceleration shows the control saturation phenomenon in the first 10 seconds, which causes the loss of guidance performance. From Figures 3(e) to 4(e), it can be seen that the estimation error of lumped disturbance rapidly converges to zero, which indicates that the NDOB can effectively estimate the real lumped disturbance. As can be seen in Figures 3(f) to 4(f), with the implementation of the proposed D-NFTSM guidance law, the missile can intercept the target successfully and have the shorter trajectory than the other trajectories for the target acceleration profiles of case 1 and case 2.

From Table 1, it can be noted that the interception time taken by the D-NFTSM, PNG and ANFTSM is comparable for all the target acceleration cases. The proposed D-NFTSM guidance law in this paper has taken shorter time than the other two guidance laws for the two cases. By comparing the miss distance, the miss distance resulting from the proposed D-NFTSM guidance law is less than the other guidance laws. So, the designed D-NFTSM guidance law has a sound and highly precise guidance performance, and it can guarantee that the missile intercepts the maneuvering target successfully.

4.2. Varying speed missiles. In the above subsection, only the simulation results for the constant speed missiles are shown. Nonetheless, as we all know, the speed of the missile for a realistic missile model is variable; hence, the following simulation results will be presented to demonstrate the effectiveness of the proposed guidance law in this paper for missiles with varying speed which is as good as that for the constant speed missiles. This is due to the inherently strong robustness of the designed guidance law. For simplicity, only a two-dimensional model is considered to design the guidance law in this paper. So, a realistic missile model [23] in the pitch plane is used to validate the effectiveness of the designed guidance law. The thrust is assumed to be a prescribed function of time. The equations of motion of a point-mass flying over a flat, non-rotating Earth are given by

$$\dot{x}_m = V_m \cos \varphi_m \quad (40)$$

$$\dot{y}_m = V_m \sin \varphi_m \quad (41)$$

$$\dot{V}_m = \frac{T - D}{m} - g \sin \varphi_m \quad (42)$$

$$\dot{\varphi}_m = \frac{a_m - g \cos \varphi_m}{V_m} \quad (43)$$

where x_m and y_m are the position of the missile; m , T and D denote the mass, the thrust and the drag of the missile, respectively.

For the realistic missile model, the aerodynamic drag D in Equation (42) is modeled as

$$D = D_1 + D_2; \quad D_1 = cq_s; \quad D_2 = \frac{km^2 a_m^2}{qs}; \quad (44)$$

$$k = \frac{1}{\pi A_r e}; \quad q = \frac{1}{2} \rho V_m^2$$

where D_1 and D_2 are the zero-lift drag and induced drag; c and k denote the zero-lift drag coefficient and the induced drag coefficient; q , A_r , e and ρ represent the dynamic pressure, the aspect ratio, the efficiency factor and the atmosphere density, respectively, and s is the reference area and assumed to be 1m^2 . For the guidance problem, the zero-lift drag coefficient and the induced drag coefficient are given as follows:

$$c = \begin{cases} 0.02 & Ma < 0.93 \\ 0.02 + 0.2(Ma - 0.93) & Ma < 1.03 \\ 0.04 + 0.06(Ma - 1.03) & Ma < 1.10 \\ 0.0442 - 0.007(Ma - 1.10) & Ma \geq 1.10 \end{cases} \quad (45)$$

$$k = \begin{cases} 0.2 & Ma < 1.15 \\ 0.2 + 0.246(Ma - 1.15) & Ma \geq 1.15 \end{cases} \quad (46)$$

where Ma is the Mach number and is given by

$$Ma = \frac{V_m}{\sqrt{1.4R_C T_P}}, \quad R_C = 288\text{J/Kkg} \quad (47)$$

where T_P is the temperature and is given by

$$T_P = \begin{cases} 288.16 - 0.006y_m & y_m < 11000 \\ 216.66 & y_m \geq 11000 \end{cases} \quad (48)$$

The thrust and the mass of the missile are given as follows:

$$T = \begin{cases} 33000 & 0 \leq t \leq 1.5 \\ 7500 & 1.5 < t \leq 8.5 \\ 0 & t \geq 8.5 \end{cases} \quad (49)$$

$$m = \begin{cases} 135 - 14.53t & 0 \leq t \leq 1.5 \\ 113.205 - 3.31(t - 1.5) & 1.5 < t \leq 8.5 \\ 90.035 & t \geq 8.5 \end{cases} \quad (50)$$

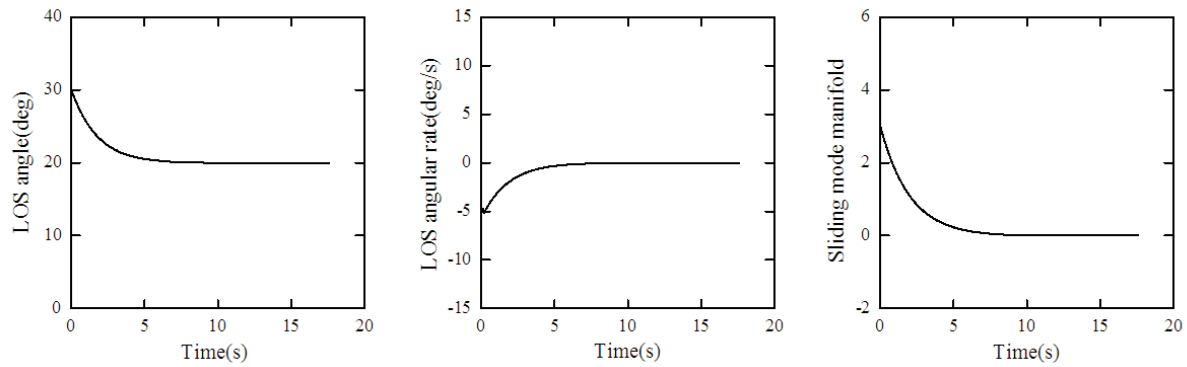
where t is time in seconds. The atmosphere density is given by

$$\rho = 1.15579 - 1.058 \times 10^{-4}y_m + 3.725 \times 10^{-9}y_m^2 - 6 \times 10^{-14}y_m^3 \quad (51)$$

The initial conditions of missile and target and the parameters of the proposed D-NFTSM guidance law (34) are chosen as the same as the previous simulation and the target acceleration is also chosen as cosine maneuvering $a_t = 7g \cos(\pi t/4) \text{m/s}^2$, which is the same as the case 1. With the implement of the proposed D-NFTSM guidance law, the LOS angle, the LOS angular rate, sliding mode manifold, missile acceleration command variation of the missile speed, estimation error of the lumped disturbance and the trajectories of missile and target are given in Figures 5(a)-5(g).

From Figures 5(a)-5(c), it can be seen that, under the proposed D-NFTSM guidance law, the LOS angle, the LOS angular rate and the sliding mode manifold could also converge to their corresponding desired values in finite time. We can observe from Figure 5(d) that the missile acceleration is less than the maximum practicable acceleration. From Figure 5(e), it can be observed that, owing to the larger thrust compared with the drag, the speed of the missile fast increases at the start of the engagement. However, the speed of the missile decreases when the thrust is less than the drag on the missile. As the missile speed decreases, the interception time for varying speed missiles is longer than that for constant missiles. As shown in Figure 5(f), it can be seen that the NDOB can track the real lumped disturbance precisely. The trajectories of the missile and the target are shown in Figure 5(g), which demonstrate that the proposed guidance law can ensure that the realistic missile intercepts the maneuvering target successfully. From the above analysis, it can be known that the designed D-NFTSM guidance law also has better guidance performance for the realistic missile intercepting the maneuvering target.

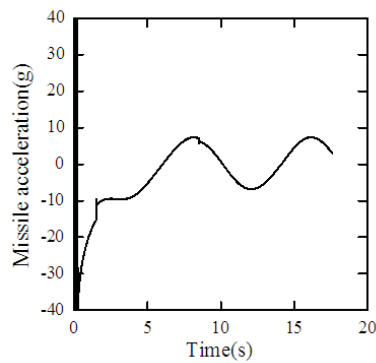
5. Conclusions. In this paper, we designed a new NDOB-based nonsingular fast terminal sliding mode guidance law with impact angle constraints for the terminal guidance problem of missiles intercepting the maneuvering targets. The proposed guidance law employs the NDOB to estimate the external disturbance, which is used to compensate the actual external disturbance; and it proposes a fast terminal sliding mode control strategy for guidance system to eliminate the singularity problem by using the saturation function. By the developed control strategy, the guidance law can guarantee that the guidance system states reach to the fast terminal sliding mode surface in finite time and converge to zero along the fast terminal sliding mode surface in finite time. The effectiveness of the proposed guidance law is verified by the numerical simulations which include the constant speed and the varying speed missile against the maneuvering target.



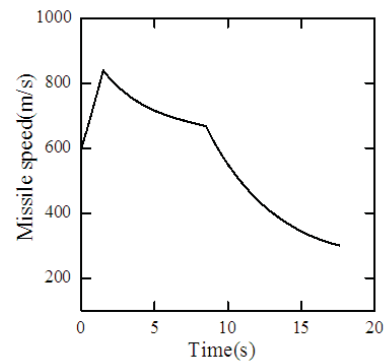
(a) LOS angle

(b) LOS angular rate

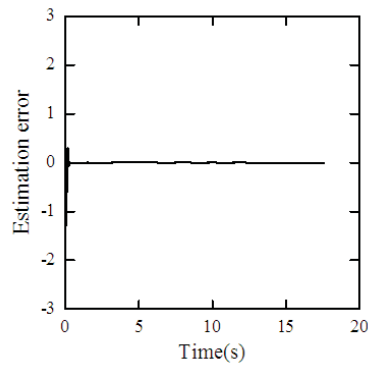
(c) Sliding mode manifold



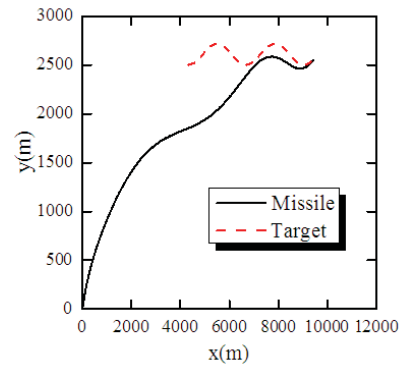
(d) Missile acceleration command



(e) Variation of the missile speed



(f) Estimation error of disturbance



(g) Trajectories of missile and target

FIGURE 5. Responses under the proposed guidance law for the varying speed missile

Acknowledgment. This work is partially supported by the Foundation for Creative Research Groups of the National Natural Science Foundation of China under Grant No.61021002. The authors also gratefully acknowledge the helpful comments and suggestions of the reviewers, which have improved the presentation.

REFERENCES

- [1] S. Rogers, Missile guidance comparison, *AIAA Guidance, Navigation, and Control Conference and Exhibit*, 2004.
- [2] C. H. Lee, T. H. Kim and M. J. Tahk, Interception angle control guidance using proportion navigation with error feedback, *Journal of Guidance, Control, and Dynamics*, vol.36, no.5, pp.1556-1561, 2013.

- [3] A. Ratnoo and D. Ghose, Impact angle constrained guidance against nonstationary nonmaneuvering targets, *Journal of Guidance, Control, and Dynamics*, vol.33, no.1, pp.269-275, 2010.
- [4] Y. I. Lee, S. H. Kim and M. J. Tahk, Optimality of linear time-varying guidance for impact angle control, *IEEE Trans. Aerospace and Electronic Systems*, vol.48, no.4, pp.2802-2817, 2012.
- [5] C. K. Ryoo, H. Cho and M. J. Tahk, Optimal guidance laws with terminal impact angle constraint, *Journal of Guidance, Control, and Dynamics*, vol.28, no.4, pp.724-732, 2005.
- [6] V. Shaferman and T. Shima, Linear quadratic guidance law for imposing a terminal intercept angle, *Journal of Guidance, Control, and Dynamics*, vol.31, no.5, pp.1400-1412, 2008.
- [7] S. Kang and H. J. Kim, Differential game missile guidance with impact angle and time constraints, *Proc. of the 18th IFAC World Congress*, pp.3920-3925, 2011.
- [8] N. Harl and S. N. Balakrishnan, Impact time and angle guidance with sliding mode control, *IEEE Trans. Control Systems Technology*, vol.20, no.6, pp.1436-1449, 2012.
- [9] T. Yamasaki, S. N. Balakrishnan, H. Takano et al, Second order sliding mode-based intercept guidance with uncertainty and disturbance compensation, *AIAA Guidance, Navigation, and Control Conference*, 2013.
- [10] S. Rao and D. Ghose, Sliding mode control based terminal impact angle constrained guidance laws using dual sliding surfaces, *Proc. of the 12th International Workshop on Variable Structure Systems*, pp.325-330, 2012.
- [11] S. R. Kumar, S. Rao and D. Ghose, Sliding-mode guidance and control for all-aspect interceptors with terminal angle constraints, *Journal of Guidance, Control, and Dynamics*, vol.35, no.4, pp.1230-1246, 2012.
- [12] L. Wu, P. Shi and H. Gao, State estimation and sliding mode control of Markovian jump singular systems, *IEEE Trans. Automatic Control*, vol.55, no.5, pp.1213-1219, 2010.
- [13] P. Shi, Y. Xia, G. Liu and D. Rees, On designing of sliding mode control for stochastic jump systems, *IEEE Trans. Automatic Control*, vol.51, no.1, pp.97-103, 2006.
- [14] J. Zhang, P. Shi and Y. Xia, Robust adaptive sliding mode control for fuzzy systems with mismatched uncertainties, *IEEE Trans. Fuzzy Systems*, vol.18, no.4, pp.700-711, 2010.
- [15] Y. B. Shtessel, I. A. Shkolnikov and A. Levant, Guidance and control of missile interceptor using second-order sliding modes, *IEEE Trans. Aerospace and Electronic Systems*, vol.45, no.1, pp.110-124, 2009.
- [16] C. Liu, Z. J. Zou and J. C. Yin, Path following and stabilization of underactuated surface vessels based on adaptive hierarchical sliding mode, *International Journal of Innovative Computing, Information and Control*, vol.10, no.3, pp.909-918, 2014.
- [17] Z. Man, A. P. Paplinski and H. R. Wu, A robust MIMO terminal sliding mode control scheme for rigid robotic manipulators, *IEEE Trans. Automatic Control*, vol.39, no.12, pp.2464-2469, 1994.
- [18] S. Sun, D. Zhou and W. T. Hou, A guidance law with finite time convergence accounting for autopilot lag, *Aerospace Science and Technology*, vol.25, no.1, pp.132-137, 2013.
- [19] Y. X. Zhang, M. W. Sun and Z. Q. Chen, Finite-time convergent guidance law with impact angle constraint based on sliding-mode control, *Nonlinear Dynamics*, vol.70, no.1, pp.619-625, 2012.
- [20] Y. Feng, X. H. Yu and Z. H. Man, Non-singular terminal sliding mode control of rigid manipulators, *Automatica*, vol.38, no.12, pp.2159-2167, 2002.
- [21] L. Y. Wang, T. Y. Chai and L. F. Zhai, Neural-network-based terminal sliding mode control of robotic manipulators including actuator dynamics, *IEEE Trans. Industrial Electronics*, vol.56, no.9, pp.3296-3304, 2009.
- [22] Y. Feng, X. H. Yu and F. L. Han, On nonsingular terminal sliding-mode control of nonlinear systems, *Automatica*, vol.49, no.6, pp.1715-1722, 2013.
- [23] S. R. Kumar, S. Rao and D. Ghose, Nonsingular terminal sliding mode guidance with impact angle constraints, *Journal of Guidance, Control, and Dynamics*, vol.37, no.4, pp.1114-1130, 2014.
- [24] S. F. Xiong, W. H. Wang, X. D. Liu et al, Guidance law against maneuvering targets with intercept angle constraint, *ISA Transactions*, 2014.
- [25] S. M. He and D. F. Lin, Adaptive nonsingular sliding mode based guidance law with terminal angular constraint, *International Journal of Aeronautical and Space Sciences*, vol.15, no.2, pp.146-152, 2014.
- [26] X. H. Yu and Z. H. Man, Fast terminal sliding mode control design for nonlinear dynamical systems, *IEEE Trans. Circuits and Systems Part I*, vol.49, no.2, pp.261-264, 2002.
- [27] S. H. Yu, X. H. Yu and B. Shirinzadeh et al, Continuous finite-time control for robotic manipulators with terminal sliding mode, *Automatica*, vol.41, no.11, pp.1957-1964, 2005.
- [28] K. Ohishi, M. Nakao and K. Miyachi, Microprocessor-controlled DC motor for load-insensitive position servo system, *IEEE Trans. Industrial Electronics*, vol.34, no.1, pp.44-49, 1987.

- [29] M. Liu, P. Shi, L. Zhang and X. Zhao, Fault tolerant control for nonlinear Markovian jump systems via proportional and derivative sliding mode observer, *IEEE Trans. Circuits and Systems I: Regular Papers*, vol.58, no.11, pp.2755-2764, 2011.
- [30] Z. Chao, A. Tsourdos and M. Lone, Disturbance observer based sliding mode controller design for large civil aircraft, *AIAA Guidance, Navigation, and Control Conference*, 2013.
- [31] K. Kim, K. Rew and S. Kim, Disturbance observer for estimating higher order disturbance in time series expansion, *IEEE Trans. Automatic Control*, vol.55, no.8, pp.1905-1911, 2010.
- [32] Z. Zhu, D. Xu, J. M. Liu et al, Missile guidance law based on extended state observer, *IEEE Trans. Industrial Electronics*, vol.60, no.12, pp.5882-5891, 2013.
- [33] K. M. Ma, H. K. Khalil and Y. Yao, Guidance law implementation with performance recovery using an extended high-gain observer, *Aerospace Science and Technology*, vol.24, no.1, pp.177-186, 2013.
- [34] Z. X. Zhang, S. H. Li and S. Luo, Composite guidance laws based on sliding mode control with impact angle constraint and autopilot lag, *Transactions of the Institute of Measurement and Control*, vol.35, no.6, pp.764-776, 2013.
- [35] Y. B. Shtessel, I. A. Shkolnikov and A. Levant, Smooth second-order sliding modes: Missile guidance application, *Automatica*, vol.43, no.8, pp.1470-1476, 2007.
- [36] P. Li, X. F. Peng, J. J. Ma et al, Non-homogeneous disturbance observer-based second order sliding mode control for a tailless aircraft, *Chinese Automation Congress*, pp.120-125, 2013.
- [37] D. Zhou, S. Sun and K. L. Teo, Guidance laws with finite time convergence, *Journal of Guidance, Control, and Dynamics*, vol.32, no.6, pp.1838-1846, 2009.
- [38] A. Levant, Higher-order sliding modes, differentiation and output-feedback control, *International Journal of Control*, vol.76, no.9, pp.924-941, 2003.